

GLOBAL STRINGS IN EXTRA DIMENSIONS: THE FULL MAP OF SOLUTIONS, MATTER TRAPPING, AND THE HIERARCHY PROBLEM

K. A. Bronnikov^a, B. E. Meierovich^{b}*

^a*Center for Gravitation and Fundamental Metrology, VNIIMS
119361, Moscow, Russia*

*Institute of Gravitation and Cosmology, PFUR
117198, Moscow, Russia*

^b*Kapitza Institute for Physical Problems
117334, Moscow, Russia*

Received August 6, 2007

We consider $(d_0 + 2)$ -dimensional configurations with global strings in two extra dimensions and a flat metric in d_0 dimensions, endowed with a warp factor $e^{2\gamma}$ depending on the distance l from the string center. All possible regular solutions of the field equations are classified by the behavior of the warp factor and the extra-dimensional circular radius $r(l)$. Solutions with $r \rightarrow \infty$ and $r \rightarrow \text{const} > 0$ as $l \rightarrow \infty$ are interpreted in terms of thick brane-world models. Solutions with $r \rightarrow 0$ as $l \rightarrow l_c > 0$, i.e., those with a second center, are interpreted as either multi-brane systems (which is appropriate for large enough distances l_c between the centers) or as Kaluza–Klein-type configurations with extra dimensions invisible due to their smallness. In the case of the Mexican-hat symmetry-breaking potential, we build the full map of regular solutions on the (ε, Γ) parameter plane, where ε acts as an effective cosmological constant and Γ characterizes the gravitational field strength. The trapping properties of candidate brane worlds for test scalar fields are discussed. Good trapping properties for massive fields are found for models with increasing warp factors. Kaluza–Klein-type models are shown to have nontrivial warp factor behaviors, leading to matter particle mass spectra that seem promising from the standpoint of hierarchy problems.

PACS: 04.50.+h, 11.27.+d

1. INTRODUCTION

The multidimensional gravity concept, tracing back to the pioneering papers by Kaluza and Klein [1], initially assumed that the extra dimensions remain unobservable due to their extreme smallness. Another class of multidimensional theories has been put forward in the 1980s, based on the idea that we live on a distinguished surface (brane) embedded in a higher-dimensional manifold, called the bulk [2]. This idea has recently become very popular in attempts to find an approach to a number of fundamental physical problems. The brane-world concept is broadly discussed in connection with the recent developments

in supersymmetric string/M-theories [3]. The simple Randall–Sundrum first model [4] continued numerous attempts [5] to find the origin of the enormous hierarchy of energy/mass scales observed in nature, which is a long-standing problem in particle physics. In astrophysics and cosmology, there are attempts to explain the dark matter and dark energy effects, to describe black holes and possible variation of fundamental constants, the CMB anisotropy, etc.

A great variety of brane-world models may be found in the literature: branes in five or more dimensions, single or multiple branes, flat or curved branes, flat or curved bulk, compact or non-compact bulk (i.e., large or infinite extra dimensions), thin or thick branes, various symmetries of both bulks and branes, different kinds of matter forming the brane, etc.

*E-mail: meierovich@yahoo.com

In our view, the most natural physical idea leading to the emergence of distinguished surfaces in the space–time manifold is the idea of a phase transition with spontaneous symmetry breaking (SSB), which has already led to great success in many areas of physics and cosmology. In other words, it is reasonable to regard the brane world as a result of a phase transition at a very early stage of the Universe evolution. The existing macroscopic theory of phase transitions with SSB allows considering the brane-world concept self-consistently and avoiding the influence of model assumptions to the largest degree, even without a detailed knowledge of the nature of the physical vacuum. A necessary consequence of such phase transitions is the appearance of topological defects.

We recall that a decisive step toward cosmological applications of the SSB concept was made in 1972 by Kirzhnits [6]. He assumed that as in the case of solid substances, a symmetry of a field system, existing at sufficiently high temperatures, could be spontaneously broken as the temperature decreases. The first quantitative analysis of the cosmological consequences of SSB was given in [7].

The properties of global topological defects are generally described with the aid of a multiplet of scalar fields playing the role of an order parameter. If a defect is to be interpreted as the origin of a brane world, its structure is determined by the self-gravity of a scalar field system and can be described by a set of Einstein and scalar equations.

This approach to the brane-world concept has been used by many authors for construction of thick branes in five (see, e.g., [8–14]) and more (see, e.g., [15–18] and the references therein) dimensions.

In our previous papers [13, 14, 17, 18], we have analyzed the gravitational properties of candidate (thick) brane worlds with the d_0 -dimensional Minkowski metric and global topological defects in $d_1 + 1$ extra dimensions. Our general formulation covered particular cases such as a brane (domain wall) in five-dimensional space–time (one extra dimension), a global cosmic string with winding number $n = 1$ (two extra dimensions), and global monopoles (three or more extra dimensions). We restricted ourselves to Minkowski branes because most of the existing problems are already clearly seen in these comparatively simple systems; on the other hand, in the majority of physical situations, the intrinsic curvature of the brane itself is much smaller than the curvature related to brane formation, and therefore the main qualitative features of Minkowski branes should survive in realistic curved branes.

Our treatment differed from many others (e.g., [15, 16]) in that we have considered all kinds of regular solutions of the corresponding field equations, including those with increasing warp factors, whose good trapping properties we have emphasized.

We have shown, in particular, that there are seven classes of regular solutions of the field equations describing global strings and monopoles in extra dimensions; two of them exist for monopoles only, while the other five are found for both strings and monopoles. Some of these configurations have exponentially increasing warp factors ($e^{2\gamma}$ in metric (1), see below) at large distances from the core. They are shown to trap linear test scalar fields of any mass and momentum. Others, ending with a flat metric, have a warp factor tending to a constant value, determined by the shape of the symmetry-breaking potential. They are also shown to trap test scalar fields with masses restricted from above by a value depending on the particular parameters of the topological defect.

Although the general classification in [17, 18] covers all possible regular configurations, the important question of the location of different solutions in the space of physical parameters remained open. One of the goals of this paper is to answer this question in the particular case of a global string in two extra dimensions and a Mexican-hat symmetry-breaking potential. The problem then contains two essential physical parameters: ε , the dimensionless cosmological constant, and Γ , characterizing the gravitational field strength. In the (ε, Γ) plane, the border lines separating different classes of regular solutions (those extending to infinite circular radii r , those with a cylindrical geometry far from the center, and those with two regular centers), are found numerically, and the asymptotic dependences $\varepsilon(\Gamma)$ as $\Gamma \rightarrow 0$ and $\Gamma \rightarrow \infty$ are derived analytically.

Another goal is to give a more complete description of the configurations of interest described by these solutions. We describe the trapping properties of different thick brane-world models for classical particles, scalar fields, and gravity. We also argue that one of the classes of regular configurations, those with two centers, can lead to promising models with nontrivial particle mass spectra. The point is that the warp factors of such configurations can have several minima at different levels, where test particles and fields may be gravitationally trapped with different energies. In this case, however, we should abandon the brane-world concept and admit that the extra dimensions are invisible due to their smallness, i.e., interpret the solutions in the spirit of Kaluza–Klein theories.

There is a growing number of publications devoted

to brane worlds with two extra dimensions (see [19] and the references therein). In many cases, the results are obtained numerically using simplified models with specially chosen sets of parameters. In our macroscopic approach, based on the theory of phase transitions with SSB, we try to reduce the influence of model assumptions to a minimum and to cover the full range of possibilities. Our main result, the full map of regular solutions for a system with the Mexican-hat symmetry-breaking potential $V(\phi)$, should probably retain its basic qualitative features for other potentials with a similar arrangement of extremum points.

The paper is organized as follows. In Sec. 2, we outline the problem setting, including the geometry, field equations, and boundary conditions providing space-time regularity. In Sec. 3, we describe the simplest solutions with a constant scalar field, needed for comparison in what follows. Section 4 is central in the paper: we give a general description and classification of possible regular solutions on the basis of our previous work [17, 18] and present a map showing the location of different solutions with the Mexican-hat potential in the parameter space of the problem. In Secs. 5 and 6, we describe some further details of the solutions and analytically derive the asymptotic behavior of the curves drawn in the map. In Sec. 7, we discuss the trapping properties of thick branes described by the above solutions. The properties of configurations with two centers are outlined in Sec. 8, and Sec. 9 is a conclusion.

2. PROBLEM SETTING

2.1. Geometry and regularity conditions

Our main interest here is a $6D$ space-time with a cosmic string in the two extra dimensions. But we begin with a more general geometry: we consider a $(D = d_0 + d_1 + 1)$ -dimensional space-time with the structure $\mathbb{M}^{d_0} \times \mathbb{R}_u \times \mathbb{S}^{d_1}$ and the metric

$$ds^2 = e^{2\gamma(u)} \eta_{\mu\nu} dx^\mu dx^\nu - \left(e^{2\alpha(u)} du^2 + e^{2\beta(u)} d\Omega^2 \right), \quad (1)$$

where

$$\eta_{\mu\nu} = \text{diag}(1, -1, \dots, -1)$$

is the d_0 -dimensional Minkowski metric ($d_0 > 1$), $d\Omega$ is a linear element on the d_1 -dimensional unit sphere \mathbb{S}^{d_1} , and α , β , and γ are functions of the radial coordinate u with the definition domain $\mathbb{R}_u \subseteq \mathbb{R}$ to be specified later. We also use the notation $r \equiv e^\beta$, where r is the spherical (circular for $d_1 = 1$) radius.

The Riemann tensor $R^{AB}{}_{CD}$ is diagonal with respect to pairs of indices and has the nonzero components

$$\begin{aligned} R^{\mu\nu}{}_{\rho\sigma} &= -e^{-2\alpha} \gamma'^2 \delta^{\mu\nu}{}_{\rho\sigma}, \\ R^{ab}{}_{cd} &= (e^{-2\beta} - e^{-2\alpha} \beta'^2) \delta^{ab}{}_{cd}, \\ R^{u\mu}{}_{u\nu} &= -\delta_\nu^\mu e^{-\gamma-\alpha} (e^{\gamma-\alpha} \gamma')', \\ R^{ua}{}_{ub} &= -\delta_b^a e^{-\beta-\alpha} (e^{\beta-\alpha} \beta')', \\ R^{a\mu}{}_{b\nu} &= -\delta_\nu^\mu \delta_b^a e^{-2\alpha} \gamma' \beta', \end{aligned} \quad (2)$$

where

$$\delta^{\mu\nu}{}_{\rho\sigma} = \delta_\rho^\mu \delta_\sigma^\nu - \delta_\sigma^\mu \delta_\rho^\nu$$

and similarly for other indices. The indices μ, ν, \dots correspond to d_0 -dimensional (physical) space-time, a, b, \dots to the d_1 angular coordinates on \mathbb{S}^{d_1} , and A, B, \dots to all D coordinates.

A necessary condition of regularity is the finiteness of all algebraic invariants of the Riemann tensor. In our case, it suffices to deal with the Kretschmann scalar

$$K = R^{AB}{}_{CD} R^{CD}{}_{AB},$$

because it is a sum of squares of all nonzero $R^{AB}{}_{CD}$. Hence, all components of Riemann tensor (2) are finite in regular configurations.

In the Gaussian gauge $\alpha = 0$, with $u = l$ being the proper distance along the radial direction, the regularity conditions at $r > 0$ look very simple:

$$\beta', \quad \beta'', \quad \gamma', \quad \gamma'' \quad \text{must be finite.} \quad (3)$$

The regularity conditions at the center $r = 0$ follow from the finiteness of the Riemann tensor component $R^{ab}{}_{cd}$ and coincide with the regular-center conditions in the usual static, spherically symmetric metrics. In terms of an arbitrary coordinate u , the regular-center conditions are

$$\gamma = \gamma_c + O(r^2), \quad e^{\beta-\alpha} |\beta'| = 1 + O(r^2) \quad \text{as } r \rightarrow 0. \quad (4)$$

The last condition insures the correct ($= 2\pi$) circumference-to-radius ratio, or, equivalently, $dr^2 = dl^2$; γ_c is a constant that can be set equal to zero by rescaling the coordinates x^μ .

The string case $d_1 = 1$ has a specific feature: there is only one angular coordinate, and therefore $\delta^{ab}{}_{cd} \equiv 0$, whence $R^{ab}{}_{cd} \equiv 0$. However, a conical singularity (i.e., an angular deficit, $dr^2 < dl^2$, or excess, $dr^2 > dl^2$) is possible, which is a pointwise, delta-like curvature peak over this zero level, as in the case of an ordinary cone top. Its existence actually means that there is some

pointlike object with respect to the two extra dimensions, or a thin brane in the space–time as a whole.

In what follows we consider entirely regular configurations, excluding conical singularities among others.

2.2. Topological defects. Field equations

A global defect with a nonzero topological charge can be constructed with a multiplet of $d_1 + 1$ real scalar fields ϕ^k , in the same way as, e.g., in [17]. It comprises a “hedgehog” configuration in $\mathbb{R}_u \times \mathbb{S}^{d_1}$:

$$\phi^k = \phi(u)n^k(x^a),$$

where n^k is a unit vector in the $(d_1 + 1)$ -dimensional Euclidean target space of the scalar fields:

$$n^k n^k = 1.$$

The total Lagrangian of the system is taken in the form

$$L = \frac{R}{2\kappa^2} + \frac{1}{2}g^{AB}\partial_A\phi^k\partial_B\phi^k - V(\phi), \quad (5)$$

where R is the D -dimensional scalar curvature, κ^2 is the D -dimensional gravitational constant, and V is a symmetry-breaking potential depending on $\phi^2(u) = \phi^a\phi^a$.

The case where $d_1 = 0$, with only one extra dimension, is a flat domain wall. Regular thick Minkowski branes supported by scalar fields with arbitrary potentials were analyzed in [13, 14].

The case where $d_1 = 1$ is a global cosmic string with the winding number $n = 1$, to be discussed here in detail. In the case $d_1 > 2$, we have a global monopole in the extra space-like dimensions (see, e.g., [15–18, 20, 21]).

We write the scalar field equation and three components of the Einstein equations for such systems in the Gaussian gauge $\alpha = 0$, $u = l$ (the prime denotes d/dl):

$$\phi'' + (d_0\gamma' + d_1\beta'^2)\phi' - d_1e^{-2\beta}\phi = \frac{\partial V}{\partial\phi}, \quad (6)$$

$$\gamma'' + d_0\gamma'^2 + d_1\beta'\gamma' = -\frac{2\kappa^2}{D-2}V, \quad (7)$$

$$\begin{aligned} \beta'' + d_0\beta'\gamma' + d_1\beta'^2 &= \\ &= (d_1 - 1 - k^2\phi^2)e^{-2\beta} - \frac{2\kappa^2}{D-2}V, \end{aligned} \quad (8)$$

$$\begin{aligned} (d_1\beta' + d_0\gamma')^2 - d_0\gamma'^2 - d_1\beta'^2 &= \\ = \kappa^2(\phi'^2 - 2V) + d_1e^{-2\beta}(d_1 - 1 - \kappa^2\phi^2). \end{aligned} \quad (9)$$

Any three of the above four equations are independent, and the fourth is their consequence.

2.3. Boundary conditions and fine-tuning relations

The metric can be rewritten in the form

$$ds^2 = e^{2\gamma(l)}\eta_{\mu\nu}dx^\mu dx^\nu - dl^2 - r^2(l)d\Omega^2, \quad (10)$$

where $r = e^\beta$ is the spherical radius. Assuming that there is a regular center ($r = 0$), we set $l = 0$ at the center without loss of generality; we classify the relevant configurations by the limit value of $r(l)$ (infinite, finite, or zero) at the largest or infinite values of l .

In the general monopole case, the regular-center condition leads to the following boundary conditions for Eqs. (6)–(9) at $l = 0$:

$$\phi(0) = \gamma'(0) = r(0) = 0, \quad r'(0) = 1. \quad (11)$$

System (6)–(9) does not contain γ but only its derivatives. For numerical integration, it is convenient to work with Eqs. (6)–(8) solved for the second-order derivatives and regard (9) as their first integral.

We thus have four boundary conditions (11) for the (effectively) fourth-order set of equations. It might seem that we must obtain a unique solution. But this is not the case because $l = 0$, being a singular point of the spherical coordinate system (not to be confused with a space–time curvature singularity), is also a singular point of our set of equations. As a result, our set of equations admits an additional freedom of choosing $\phi'(0)$; or, instead, we may use the requirement of global regularity to obtain a unique solution.

2.3.1. Infinite extra dimensions

If the solution is defined in the interval $0 \leq l < \infty$, then the lacking boundary condition can be taken as $\phi \rightarrow \text{const}$ as $l \rightarrow \infty$, or

$$\phi'(\infty) = 0. \quad (12)$$

In general, when the scalar field starts from a maximum of the potential and ends at a finite value of ϕ , the five boundary conditions in (11) and (12) uniquely determine a nontrivial solution of our field equations. Its existence determines a certain area in the space of parameters of the problem without *a priori* fine tuning. An asymptotic analysis at $l \rightarrow \infty$ shows that in this general case, $\beta(l)$ is a linearly increasing function as $l \rightarrow \infty$, and $r'(\infty) \geq 0$.

$r'(\infty) = 0$ is the special case, where r tends to a finite constant as $l \rightarrow \infty$. The solution then terminates at a slope of the potential rather than at its minimum. The supplementary condition $r'(\infty) = 0$ seems to require a fine-tuning relation between the free parameters

of the problem. But we see in what follows that it is not quite so. An analysis of solutions with $\phi = \phi_0 = \text{const}$ shows that there is also an area in the parameter space where condition (12) is satisfied automatically, and solutions with $r'(l) \rightarrow 0$ as $l \rightarrow \infty$ exist without any fine tuning.

2.3.2. Two centers

It can happen that the integral curves of a solution terminate at some finite value l_c with $r(l_c) = 0$ and $\phi(l_c) = 0$, which is one more center. Of interest for us are configurations in which this second center $l = l_c$ is also regular. Then the same four conditions (11) must also hold at $l = l_c$. Two of them can be satisfied by choosing the values of $\phi'(0)$ and l_c . The other two can only be satisfied by a proper choice of free (input) parameters of the problem, e.g., those of the potential (if any) and the cosmological constant.

In the special case of symmetry between the centers¹⁾, the input parameters are connected by only one fine-tuning relation. In this case, the boundary conditions at the second center are satisfied automatically, and the existence of a regular solution is provided by three conditions of smoothness at the middle (equator) point $l_{eq} = l_c/2$:

$$\phi'(l_{eq}) = \gamma'(l_{eq}) = r'(l_{eq}) = 0.$$

Two of these three conditions determine the values of l_c and $\phi'(0)$, and the remaining one requires fine tuning of the input parameters of the problem.

The fine tuning could be avoided at the expense of admitting conical singularities (in the string case) at the two centers. For symmetric solutions, the three smoothness conditions at the equator can be satisfied by choosing $\phi'(0)$, $r'(0)$, and l_c . In the general case of

¹⁾ Equations (6)–(9) are invariant under translations $l \rightarrow l + l_0$ and under reflections $l_0 + l \rightarrow l_0 - l$, $\phi \rightarrow -\phi$. This invariance leads to the existence of regular solutions with two centers, which are symmetric with respect to the middle point [17]. Furthermore, a solution with two regular centers defined in the interval $(0, l_c)$ can be symmetrically extended to the next interval $(l_c, 2l_c)$ and further on, thus leading to a periodic solution for $l \in \mathbb{R}$ [22]. The metric remains regular everywhere, but the points of contacts $(0, \pm l_c, \pm 2l_c, \dots)$ are geometrically ambiguous: each of them belongs to two adjacent manifolds simultaneously. If one still believes in the reality of such systems, one can note that the spectrum of a low-energy particle in a perfectly periodic potential has a conductivity zone, allowing free propagation and thus making the extra dimension observable in principle. However, if the conductivity zone is very narrow, then even small perturbations should lead to localization of a particle. This interesting new possibility is worth a special consideration.

nonsymmetric centers, the four conditions of the second center can be satisfied by appropriately choosing $\phi'(0)$, $r'(0)$, $r'(l_c)$, and l_c .

2.4. String equations

In the string case $d_1 = 1$, to be considered here in detail, the field equations become

$$\phi'' + (d_0\gamma' + \beta'^2)\phi' - e^{-2\beta}\phi = \frac{\partial V}{\partial \phi}, \tag{13}$$

$$\gamma'' + d_0\gamma'^2 + \beta'\gamma' = -\frac{2\chi^2}{d_0}V, \tag{14}$$

$$\beta'' + d_0\beta'\gamma' + \beta'^2 = -(\chi^2\phi^2)e^{-2\beta} - \frac{2\chi^2}{d_0}V, \tag{15}$$

$$2d_0\gamma'\beta' + d_0(d_0 - 1)\gamma'^2 = \chi^2(\phi'^2 - 2V) - \chi^2\phi^2e^{-2\beta}. \tag{16}$$

For numerical examples, we use the so-called Mexican-hat potential

$$V = \frac{1}{4}\lambda_0\eta^4 \left[\varepsilon + \left(1 - \frac{\phi^2}{\eta^2} \right)^2 \right]. \tag{17}$$

The parameter ε plays the role of a cosmological constant added to the conventional Mexican-hat potential (the “hat” is thus moved up or down). To pass to dimensionless quantities, we put $\lambda_0\eta^2 = 1$, and hence lengths are measured in units of $1/\sqrt{\lambda_0}\eta$, which in many cases has the meaning of the string core radius²⁾.

The potential then takes the form

$$V = \frac{1}{4}\eta^2[\varepsilon + (1 - f^2)^2], \quad f := \frac{\phi}{\eta}. \tag{18}$$

The remaining free parameters that control the system behavior are

$$d_0, \quad \varepsilon, \quad \text{and} \quad \Gamma := \chi^2\eta^2. \tag{19}$$

We use $d_0 = 4$ in computations. The parameter Γ characterizes the gravitational field strength.

To further describe different regular solutions of our field equations, we begin with the simplest solutions where $\phi = \phi_* = \text{const}$. They are not string solutions but are helpful for comparison.

²⁾ From the very beginning, we put $c = \hbar = 1$, and therefore all quantities are measured in appropriate powers of length $[\ell]$. Then some relevant dimensionalities are $[V] = [\ell^{-D}]$, $[\phi^2] = [\eta^2] = [\chi^{-2}] = [\ell^{2-D}]$.

3. SOLUTIONS WITH $\phi = \text{const}$

If $\phi = \phi_* = \text{const}$, we are actually dealing with vacuum field equations for metric (10) with the cosmological constant $\Lambda = \varkappa^2 V(\phi_*)$. Scalar field equation (13) then reduces to

$$\frac{\phi_*}{r^2} = -V_\phi(\phi_*), \quad V_\phi := \frac{dV}{d\phi}. \tag{20}$$

This leads to two kinds of solutions: one exists in the case where $V_\phi(\phi_*) = 0$ and $\phi_* = 0$, and the other corresponds to $V_\phi(\phi_*) \neq 0$ (i.e., ϕ is “frozen” on a slope of the potential), and we should put $r = \text{const}$ in this case.

For potential (17), Eq. (20) gives

$$f_*(r^{-2} - 1 + f_*^2) = 0, \tag{21}$$

and hence either

$$f_* = \frac{\phi_*}{\eta} = 0$$

or

$$f_*^2 = 1 - \frac{1}{r^2}.$$

3.1. Solutions with $\phi \equiv 0$

The trivial regular solutions with the order parameter $\phi = 0$ describe configurations with a higher symmetry, which can become spontaneously broken into a structure with a topological defect.

In this case, the metric satisfies the equations

$$\begin{aligned} \gamma'' + \gamma'(d_0\gamma' + \beta') &= -8\Lambda/d_0, \\ \beta'' + \beta'(d_0\gamma' + \beta') &= -8\Lambda/d_0, \\ (d_0 - 1)\gamma'^2 + 2\gamma'\beta' &= -8\Lambda/d_0. \end{aligned} \tag{22}$$

Eliminating β' , we obtain the equation for γ

$$\gamma'' + \frac{1}{2}(d_0 + 1)\gamma'^2 + \frac{4\Lambda}{d_0} = 0. \tag{23}$$

Its solutions are different for positive and negative Λ . For $\Lambda > 0$, we have (requiring $\gamma(0) = \gamma'(0) = 0$, a regular center at $l = 0$)

$$\exp[(d_0 + 1)\gamma] = \cos^2(\lambda_1 l), \quad \lambda_1 = \sqrt{2\Lambda \frac{d_0 + 1}{d_0}}. \tag{24}$$

For $r = e^\beta$, the last equation in (22) then gives

$$r^2 = r_0^2 \exp[-(d_0 - 1)\gamma] \sin^2(\lambda_1 l), \quad r_0 = \text{const}, \tag{25}$$

where, choosing $r_0 = 1/\lambda_1$, we can satisfy the regularity condition $r'(0) = 1$. We thus have a configuration

with a regular center but with a singularity $e^\gamma \rightarrow 0$ and $r \rightarrow \infty$ as $l \rightarrow \pi/2\lambda_1$.

For potential (17), this case corresponds to $\varepsilon > -1$.

For $\Lambda < 0$, corresponding to $\varepsilon < -1$, we have³⁾

$$e^\gamma = \text{ch}^{2/(d_0+1)}(\lambda_2 l), \quad \lambda_2 = \sqrt{-2\Lambda \frac{d_0 + 1}{d_0}}, \tag{26}$$

$$r = r_0 \frac{\text{sh}(\lambda_2 l)}{[\text{ch}(\lambda_2 l)]^{(d_0-1)/(d_0+1)}} \tag{27}$$

instead of (24) and (25); again, choosing $r_0 = 1/\lambda_2$, we can satisfy the regularity condition $r'(0) = 1$.

Therefore, the configuration with unbroken symmetry is completely regular and extends from the regular center $l = 0$ to $l = \infty$, where the warp factor $e^{2\gamma}$ and the radius r are infinitely increasing functions.

3.2. Solution with $\phi = \phi_* = \text{const} \neq 0$

In this case, Eq. (20) leads to a constant radius $r = r_*$, and Eq. (15) gives the relation

$$\frac{\phi_*^2}{r_*^2} = -\frac{V(\phi_*)}{d_0}, \tag{28}$$

whence it follows that

$$V(\phi_*) = \Lambda/\varkappa^2 < 0.$$

For γ , we use (16) to obtain

$$d_0^2 \gamma'^2 = -2\Lambda, \quad \exp(d_0 \gamma) = \exp(\pm \sqrt{-2\Lambda} l). \tag{29}$$

The coordinate range is $l \in \mathbb{R}$. In particular, for potential (17), it follows from (21) and (15) that

$$r = \frac{1}{\sqrt{1 - f_*^2}} = \text{const}, \tag{30}$$

$$\varepsilon = -2d_0(1 - f_*^2)f_*^2 - (1 - f_*^2)^2 < 0, \tag{31}$$

$$\Lambda = \varkappa^2 V(\phi_*) = -\frac{1}{2} \varkappa^2 \eta^2 d_0 f_*^2 (1 - f_*^2). \tag{32}$$

The configurations with $\phi = \text{const} \neq 0$ and $r = \text{const}$ are regular but evidently cannot be interpreted in terms of a brane world. They only provide the asymptotic behavior of the “tube” solutions presented below.

³⁾ For $d_0 = 4$, these formulas reduce to those found earlier in [23].

4. REGULAR STRING SOLUTIONS. CLASSIFICATION AND MAP IN THE (Γ, ε) PLANE

The possible types of regular solutions of our field equations were classified in Refs. [17, 18]. The table below represents this classification for the string case $d_1 = 1$. Compared to [17], this Table does not include the solutions existing only for $d_1 > 1$, but additionally includes the solutions (labelled A0 and B0) from Sec. 3.

In what follows, we deal with potential (18). For this potential, Fig. 1 presents the location of different regular string solutions in the plane of parameters (Γ, ε) . The map shows solutions with the ϕ field having a constant sign. Those with alternate signs of ϕ are discussed in Sec. 6. There are no regular string solutions at $\varepsilon > 0$.

In Fig. 1, the curve (1) is the upper boundary of the area of class-A1 solutions with $r \rightarrow \infty$ as $l \rightarrow \infty$. The points on this curve and in the whole area $-1 > \varepsilon \geq \varepsilon_*(\Gamma)$ correspond to class-B2 solutions. Fine-tuned solutions with two symmetric regular centers (see Fig. 7 below) are located along the curve (2). The class of fine-tuned solutions with a horizon (B1) is represented by the curve (3).

We briefly describe the classes of solutions presented

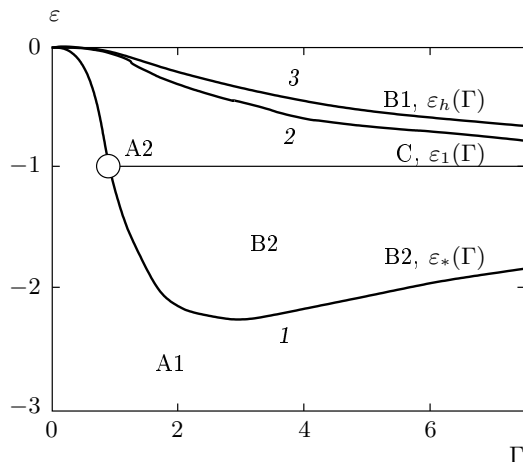


Fig. 1. Location of solutions in the plane of parameters (Γ, ε) . Curve (1), $\varepsilon_*(\Gamma)$ is the upper boundary of the area of class-A1 solutions with $r \rightarrow \infty$ as $l \rightarrow \infty$. This curve itself and the whole area $-1 > \varepsilon \geq \varepsilon_*(\Gamma)$ correspond to class-B2 solutions with $r(\infty) = \text{const}$. Fine-tuned solutions with two symmetric regular centers (class C) are located along curve (2), $\varepsilon_1(\Gamma)$. The class B1 of fine-tuned solutions with a horizon is represented by the curve (3), $\varepsilon_h(\Gamma)$

in the map, postponing the derivation of some important details of the curves to the subsequent sections.

A: Configurations with infinite r

From the Table, we can note a close similarity between the vacuum solutions A0 (where $\phi \equiv 0$) and A1. In fact, the gravitational field in both cases is mainly governed by the (negative) cosmological constant. In the limit case $|\varepsilon| \gg 1, \varepsilon < 0$, the role of the symmetry-breaking potential $V(\phi)$ is negligible. Then, as follows from (14), γ' is always positive, the warp factor $e^{2\gamma}$ increases, and gravity is attractive towards $l = 0$. These solutions with $r \rightarrow \infty$ at large l exist without any fine tuning.

As $|\varepsilon|$ decreases, the potential $V(\phi)$ becomes more and more important, and at ε approaching some $\varepsilon_*(\Gamma)$, the derivative $r' \rightarrow 0$, such that class-A1 solutions pass over to asymptotically cylindrical fine-tuned class-B2 solutions.

The main features of class-A1 solutions at large l are as follows.

- 1) The scalar field $\phi(l)$ tends to a minimum of $V(\phi)$.
- 2) The quantities $\gamma'(l)$ and $\beta'(l)$ tend to the same finite positive constant, and hence $e^{\gamma(l)} \sim r(l)$ increase exponentially.

An example of class-A1 solution, found numerically, is presented in Fig. 2.

As regards the A2 class, this is an exceptional solution corresponding to the condition $V(0) = 0$, hence $\varepsilon = -1$. In this case [18], a regular integral curve starting at $l = 0$ with $\phi = 0$ finishes again with $\phi \rightarrow 0$ as $l \rightarrow \infty$. The large- l behavior of r and of the warp factor $e^{2\gamma}$ in the resulting regular solutions is

$$r \approx l, \quad e^{d_0\gamma} \sim l.$$

B: Asymptotically cylindrical configurations

For these “tube” solutions, it is easy to verify that Eqs. (29)–(31) hold at large l and, in particular, $f \rightarrow f_* = \text{const}$ with $0 < f_*^2 < 1$.

The vacuum solution B0, with $r \equiv r_*$, actually interpolates between the cylindrical asymptotics of B1 ($e^\gamma \rightarrow 0$, a double horizon) and B2 ($e^\gamma \rightarrow \infty$ at $l \rightarrow \infty$, i.e., gravitational attraction towards the center $l = 0$).

Equation (31) does not contain \varkappa and allows finding the range of the input parameter ε for which “tube” solutions are possible. The dependence $\varepsilon(f_*)$ is shown in Fig. 3. By Eq. (31),

$$\varepsilon > \varepsilon_{min} = -1 - \frac{(d_0 - 1)^2}{2d_0 - 1}. \tag{33}$$

Classification of regular $(d_0 + 2)$ -dimensional solutions for arbitrary $V(\phi)$ by the types of asymptotic behavior at the largest or infinite l . The columns labeled by r , ϕ , and γ show their final values. Attraction or repulsion is understood with respect to the center. The symbol η denotes a minimum of $V(\phi)$

Notation	l range	r	ϕ	$V(\phi)$	γ	Asymptotic type
A0	\mathbb{R}_+	∞	$\equiv 0$	$V(0) < 0$	∞	AdS, attraction
A1	\mathbb{R}_+	∞	η	$V(\eta) < 0$	∞	AdS, attraction
A2	\mathbb{R}_+	∞	0	0	∞	power-law, attraction
B0	\mathbb{R}	$\equiv r_*$	$\equiv \phi_* \neq 0$	$V_* < 0$	$\pm\infty$	horizon at one end
B1	\mathbb{R}_+	r_*	$\phi_* \neq 0$	$V_* < 0$	$-\infty$	horizon, repulsion
B2	\mathbb{R}_+	r_*	$\phi_* \neq 0$	$V_* < 0$	∞	attracting tube
C	$(0, l_c)$	0	0	$V(0) > 0$	const	second center

For $d_0 = 4$,

$$\varepsilon_{min} = -16/7 = -2.2857\dots$$

It also follows from (31) and Fig. 3 that in the range $-1 > \varepsilon > \varepsilon_{min}$, there are two branches of the inverse function $f_*(\varepsilon)$. In the range $0 \geq \varepsilon > -1$, there is only one branch. Other limit values are expressed in terms of f_* by Eqs. (29)–(32), and

$$\gamma' \rightarrow \varkappa \eta \sqrt{d_0 f_*^2 (1 - f_*^2)}. \tag{34}$$

Class-B2 configurations occupy a whole area in the (ε, Γ) parameter plane, whereas B1 solutions require fine tuning and are located on the curve 3 in the map (see Fig. 1).

C: Configurations with two centers

As was argued above, class-C solutions can be symmetric and asymmetric with respect to reflections $l \rightarrow l_c - l$. Symmetric solutions require one fine-tuning relation, which corresponds to particular curves in the (ε, Γ) plane. The curve describing solutions with a constant sign of ϕ is presented in Fig. 1 (curve (2)). Other symmetric configurations are discussed below. Asymmetric solutions can only appear at discrete points in the parameter plane, and we do not mention them any more.

5. “TUBE” SOLUTIONS: LOCATION IN THE PARAMETER PLANE

The upper boundary $\varepsilon_*(\Gamma)$ of class-A solutions, found numerically point by point for $d_0 = 4$, is presented in Fig. 4 by the curve (1) and the circles. Any

point in the area $\varepsilon < \varepsilon_*(\Gamma)$, $0 < \Gamma < \infty$ corresponds to a class-A solution with f monotonically increasing from zero at the center to unity. The function $\varepsilon_*(\Gamma)$ decreases from zero at $\Gamma = 0$ to a minimum with $\varepsilon = \varepsilon_{min}$ in accordance with Eq. (33) and then increases tending to -1 as $\Gamma \rightarrow \infty$.

In the range $0 > \varepsilon > -1$, the “tube” (fine-tuned) solutions only exist precisely on the line $\varepsilon_*(\Gamma)$, which comprises a border between A and C classes of solutions.

In the range $-1 > \varepsilon > \varepsilon_*(\Gamma)$, there are cylindrical solutions without fine tuning. This area is located between the zones of A and C classes of solutions.

In the limits of weak and strong gravitational fields (small and large Γ , respectively), numerical analysis of the field equations is hindered, and we have derived the function $\varepsilon_*(\Gamma)$ analytically. The curve (2) in Fig. 4 corresponds to $\Gamma \ll 1$ and the curve (3) to $\Gamma \gg 1$.

5.1. Strong gravity: $\Gamma \gg 1$

As follows from the numerical analysis, the scalar field in “tube” solutions is small in this case, and the potential can be expanded in a series:

$$V(\phi) \approx V_0 + \frac{1}{2} V_0'' \phi^2, \quad \frac{dV}{d\phi} \approx V_0'' \phi.$$

The problem is completely determined by the two constants

$$V_0 = V(0)$$

and

$$V_0'' = \left(\frac{d^2 V}{d\phi^2} \right)_{\phi=0}.$$

We introduce a new parameter λ and a new function ψ :

$$\lambda = 4\varkappa^2 V_0, \quad \psi = \varkappa \phi. \tag{35}$$

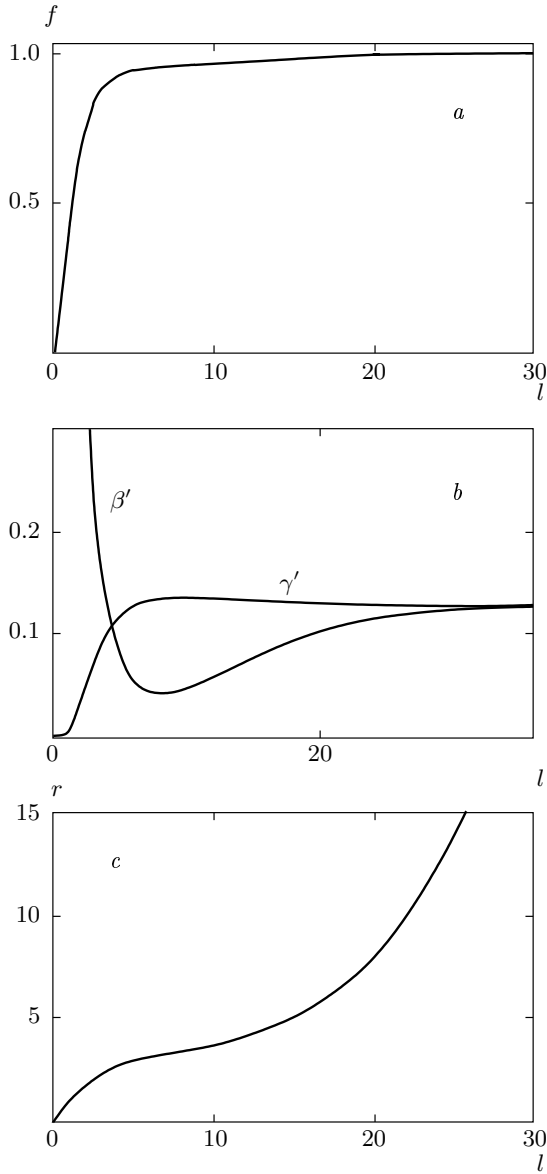


Fig. 2. An example of class-A1 solution with the parameters: $\Gamma = 0.7$, $\varepsilon = -0.9$: $f(l)$ (a); $\beta'(l)$, $\gamma'(l)$ (b); and $r(l)$ (c)

For Mexican-hat potential (17),

$$V_0 = \eta^2(\varepsilon + 1)/4,$$

and

$$V_0'' = -1,$$

and therefore

$$\lambda = \Gamma(\varepsilon + 1) \tag{36}$$

(we recall that $\Gamma := \varkappa^2 \eta^2$). Equations (13)–(15) become

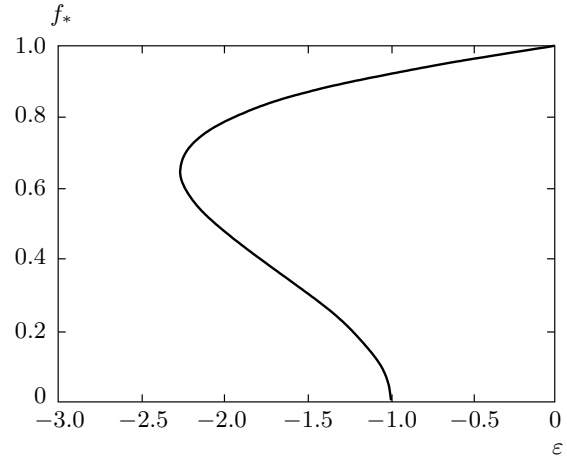


Fig. 3. The dependence $\varepsilon(f_*)$ in (31) in the case of an infinite cylinder

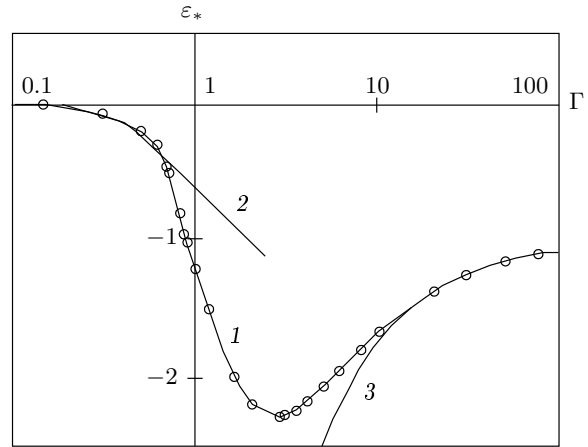


Fig. 4. The upper boundary $\varepsilon_*(\Gamma)$ of class-A1 solutions with infinite r . The points forming the curve (1) are found numerically. The asymptotic dependences at $\Gamma \ll 1$ (Eq. (49)) (curve 2) and $\Gamma \gg 1$ (Eq. (40)) (curve 3)

$$\gamma'' + \gamma'(d_0 \gamma' + \beta') = -\frac{\lambda}{2d_0} + \psi^2/d_0, \tag{37}$$

$$\beta'' + \beta'(d_0 \gamma' + \beta') = \psi^2 \left(\frac{1}{d_0} - e^{-2\beta} \right) - \frac{\lambda}{2d_0}, \tag{38}$$

$$\psi'' + \psi'(d_0 \gamma' + \beta') = \psi(e^{-2\beta} - 1), \tag{39}$$

and depend on only one dimensionless parameter λ . The boundary conditions are

$$\gamma(0) = \gamma'(0) = \psi(0) = 0, \quad (e^\beta)'|_{l=0} = 1,$$

$$\beta'(\infty) = \psi'(\infty) = 0.$$

Scalar field equation (39) is homogeneous with respect to ψ and looks linear; however, the system as a whole is nonlinear, and we have a nonlinear eigenvalue problem. The parameter d_0 being fixed, there is only one dimensionless parameter λ , whose ground-state eigenvalue is expected to be of the order of unity. In accordance with (36) for $\Gamma \gg 1$, the parameter ε is then very close to -1 , and f_0 in (31) is $\sim \Gamma^{-1} \ll 1$. It follows from (39) that $r \equiv e^\beta \rightarrow 1$ at large l . Nontrivial solutions exist for discrete values of λ , one of which, corresponding to a monotonically increasing $\psi(l)$, is found numerically:

$$\lambda = -7.433\dots, \quad d_0 = 4.$$

The asymptotic dependence $\varepsilon_*(\Gamma)$ for $\Gamma \gg 1$

$$\varepsilon = -1 + \lambda/\Gamma \tag{40}$$

is presented in Fig. 4 by the curve (3).

5.2. Weak gravity: $\Gamma \ll 1$

The case $\Gamma \ll 1$ is more complicated. A numerical computation shows (and it is verified analytically) that $|\varepsilon|$ is exponentially small as $\Gamma \rightarrow 0$. From (31), we see that

$$1 - f_0^2 \approx -\frac{\varepsilon}{2d_0} \ll 1,$$

and the limit value of circular radius (30),

$$r_* \approx \sqrt{\frac{2d_0}{|\varepsilon|}},$$

is very large compared with the “core” radius ~ 1 . The equations simplify differently in the two cases where $r \ll r_*$ and $r \gg 1$. The solutions must coincide in the intermediate region $1 \ll r \ll r_*$.

For $\Gamma \ll 1$, it is convenient to rewrite the field equations in terms of $r = e^\beta$:

$$\gamma'' = -\gamma' \left(d_0 \gamma' - \frac{r'}{r} \right) - \frac{\Gamma}{2d_0} [\varepsilon + (1 - f^2)^2], \tag{41}$$

$$r'' = \frac{(d_0 - 1)d_0}{2} \gamma'^2 r - \frac{\Gamma}{2} \frac{f^2}{r} - \frac{\Gamma}{2} f'^2 r - \frac{\Gamma}{4} [\varepsilon + (1 - f^2)^2] r, \tag{42}$$

$$f'' = -f' \left(d_0 \gamma' - \frac{r'}{r} \right) + \frac{f}{r^2} - f(1 - f^2). \tag{43}$$

For $r \ll r_*$, we see that $\gamma' \sim \Gamma \ll 1$, and the term with γ'^2 in (42) can be neglected. In the vicinity of the

center, in the terms $\sim \Gamma$, we can set $r = l$ and omit ε . Then Eq. (42) reduces to

$$r'' = -\Gamma \frac{f_0^2}{l} - \frac{\Gamma}{2d_0} (1 - f_0^2)^2 l, \quad \Gamma \ll 1, \quad l \ll r_*,$$

where f_0 is the solution of Eq. (43) with $\gamma' = 0$, $r = l$, and the boundary conditions $f(0) = 0$, $f(\infty) = 1$. With $r'(0) = 1$, integration yields

$$r' = 1 + \Gamma \left[-f_0^2 \ln l + 2 \int_0^l dl f_0 f_0' \ln l - \frac{1}{2d_0} \int_0^l dl (1 - f_0^2)^2 l \right].$$

The integrals rapidly converge for $l \gg 1$, and in the intermediate region $1 \ll l \ll r_*$ we have

$$r'^2 = 1 + 2\Gamma \left(-\ln r + 2J_2 - \frac{J_1}{2d_0} \right), \tag{44}$$

$$\Gamma \ll 1, \quad 1 \ll r \ll r_*,$$

where the integrals J_1 and J_2 are found numerically:

$$J_1 = \int_0^\infty l dl (1 - f_0^2)^2 = 1, \tag{45}$$

$$J_2 = \int_0^\infty dl f_0 f_0' \ln l \approx 0.2.$$

In the region $r \gg 1$, Eq. (42) reduces to

$$r'' = -\Gamma \left(\frac{1}{r} + \frac{\varepsilon}{2d_0} r \right), \quad \Gamma \ll 1, \quad 1 \ll r. \tag{46}$$

Taking into account that $r' = 0$ at $r = r_*$, we find

$$\frac{1}{2} r'^2 = \Gamma \left(\ln r_* - \ln r + \frac{\varepsilon}{4d_0} r_*^2 - \frac{\varepsilon}{4d_0} r^2 \right), \tag{47}$$

$$\Gamma \ll 1, \quad 1 \ll r.$$

In the intermediate region $1 \ll r \ll r_*$ we have

$$r'^2 = 2\Gamma \left(\frac{1}{2} \ln \frac{2d_0}{|\varepsilon|} - \ln r - \frac{1}{2} \right), \tag{48}$$

$$\Gamma \ll 1, \quad 1 \ll r \ll r_*.$$

We have taken into account that

$$r_* = \sqrt{\frac{2d_0}{|\varepsilon|}}.$$

Comparing (44) with (48), we find the fine-tuning relation between ε and Γ for asymptotically cylindric configurations in the weak-gravity limit:

$$\begin{aligned} \varepsilon &= -2d_0 \exp\left(-\frac{1}{\Gamma} - 4J_2 - 1 - \frac{J_1}{d_0}\right) \approx \\ &\approx -0.33 d_0 \exp\left(-\frac{1}{\Gamma} + \frac{1}{d_0}\right), \quad (49) \end{aligned}$$

$$\varepsilon \approx -1.7e^{-1/\Gamma}, \quad d_0 = 4, \quad \Gamma \ll 1.$$

This asymptotic dependence, $\varepsilon_*(\Gamma)$ for $\Gamma \ll 1$, is presented in Fig. 4 by the curve (2).

5.3. Solutions in the range $-1 > \varepsilon > \varepsilon_*(\Gamma)$

In the range $-1 > \varepsilon > \varepsilon_*(\Gamma)$, there exist class-B2 solutions ($r \rightarrow r_* < \infty$ as $l \rightarrow \infty$) without any fine-tuning relation between the parameters ε and Γ . The asymptotic values of the scalar field (f_*) and the radius (r_*) at large l are independent of Γ :

$$\begin{aligned} f_*^2 &= \frac{d_0 - 1 - \sqrt{(d_0 - 1)^2 + (\varepsilon + 1)(2d_0 - 1)}}{2d_0 - 1}, \\ r_*^2 &= \frac{2d_0 - 1}{d_0 + \sqrt{(d_0 - 1)^2 + (\varepsilon + 1)(2d_0 - 1)}}. \end{aligned}$$

An example of such a solution is shown in Fig. 5 for $\Gamma = 2$ and $\varepsilon = -1.1$. The scalar field $f(l)$ is shown in Fig. 5a, $\gamma'(l)$ and $\beta'(l)$ are shown in Fig. 5b, and $r(l)$ is displayed in Fig. 5c.

5.4. Solutions with a horizon

We consider class-B1 configurations with a horizon, with $\gamma(l)$ linearly decreasing as $l \rightarrow \infty$. Their location, found numerically, is shown in Fig. 1 by the curve (3), $\varepsilon = \varepsilon_h(\Gamma)$, corresponding to a certain fine-tuning relation. An example of such a regular solution, with the parameters $\Gamma = 2$ and $\varepsilon = -0.233846$, is presented in Fig. 6.

The near-horizon metric has the asymptotic form

$$\begin{aligned} ds^2 &= C^2 e^{-2hl} \eta_{\mu\nu} dx^\mu dx^\nu - dl^2 - r_*^2 d\Omega^2, \\ h &= \gamma'(\infty). \end{aligned} \quad (50)$$

The substitution $e^{-hl} = \rho$ (converting $l = \infty$ to a finite coordinate value, $\rho = 0$) brings metric (50) to the form

$$\begin{aligned} ds^2 &= C^2 \rho^2 \eta_{\mu\nu} dx^\mu dx^\nu - \frac{d\rho^2}{k^2 \rho^2} - r_*^2 d\Omega^2, \\ \rho &\rightarrow 0. \end{aligned} \quad (51)$$

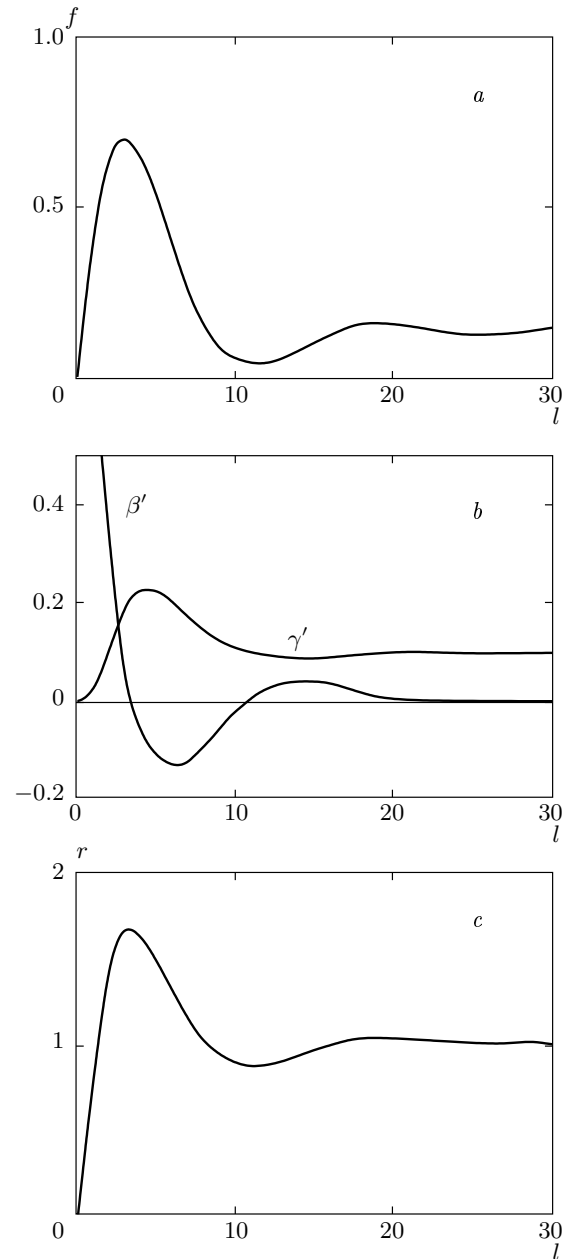


Fig. 5. An example of class-B2 solution for $\Gamma = 2$ and $\varepsilon = -1.1$: $f(l)$ (a); $\beta'(l)$, $\gamma'(l)$ (b), and $r(l)$ (c)

Therefore, $\rho = 0$ is a second-order Killing horizon in the two-dimensional subspace parametrized by t and ρ ; the extra-dimensional circular radius squared remains positive. It is of the same nature as, e.g., the extreme Reissner–Nordström black-hole horizon, or the anti-de Sitter horizon in the second Randall–Sundrum brane-world model. A peculiarity of the present horizon is that the spatial part of the metric, which takes the form $\rho^2(dx)^2$ at large l , is degenerate at $\rho = 0$. The volume of the d_0 -dimensional space–time vanishes as $l \rightarrow \infty$. It

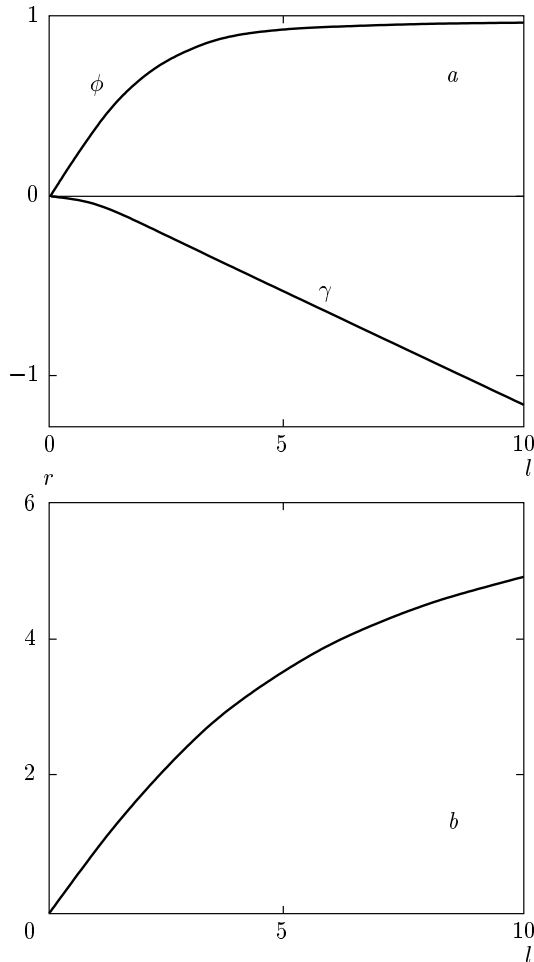


Fig. 6. An example of class-B1 solution with a horizon for $\Gamma = 2$ and $\varepsilon = -0.233846$: the scalar field ϕ and the metric function γ (a); the circular radius r (b)

remains degenerate even if we pass to Kruskal-like coordinates in the (t, ρ) subspace. But the D -dimensional curvature is finite there, indicating that a transition to negative values of ρ (where the old coordinate l is no longer applicable) is meaningful.

Thus solutions with strings (and/or monopoles) in extra dimensions may contain second-order horizons, and the degenerate nature of the spatial metric at the horizon does not lead to a curvature singularity; moreover, the metric can be continued in a Kruskal-like manner. However, the zero volume of the spatial section makes the density of any additional (test) matter infinite at $\rho = 0$. To regard these solutions as describing viable configurations, one needs to take the back-reaction of ordinary matter into account. It evidently destroys such a configuration.

6. SOLUTIONS WITH TWO REGULAR CENTERS: LOCATION IN THE PARAMETER PLANE

Symmetric class-C solutions with two regular centers are located on the (ε, Γ) plane in the region $0 > \varepsilon > -1$ to the right of the fine-tuning curve (1), $\varepsilon_*(\Gamma)$, in Fig. 4 or, which is the same, to the right of the curve (1) in the full map, Fig. 1. The solutions are fine-tuned, i.e., located along certain lines $\varepsilon_N(\Gamma)$ in this region, where N is the number of half-waves and $N - 1$ is the number of knots (zeros) of the scalar field $f = \phi/\eta$. The point is that f , just as the radius r , is zero at both centers, but f can change its sign. Therefore, there are several families of regular solutions with different numbers N of half-waves, each family corresponding to a line $\varepsilon_N(\Lambda)$ in the parameter plane. The curve (2) in Fig. 1 depicts $\varepsilon_1(\Lambda)$.

6.1. Solutions without knots of the scalar field

In solutions where f has a constant sign, all three functions $f(l)$, $r(l)$, and $\gamma(l)$ reach their extremum values at the equator $l = l_{eq}$. Setting

$$f'(l_{eq}) = r'(l_{eq}) = \gamma'(l_{eq}) = 0 \tag{52}$$

in the first integral in (16), we find a relation between $f(l_{eq}) =: f_{eq}$ and $r(l_{eq}) =: r_{eq}$:

$$r_{eq}^2 = \frac{2f_{eq}^2}{|\varepsilon| - (1 - f_{eq}^2)^2}. \tag{53}$$

It is convenient to use (53) together with (52) as boundary conditions and perform numerical integration from the equator to one of the centers. Then the three conditions $f(l_c) = 0$, $r(l_c) = 0$, and $r'(l_c) = 1$ determine the values of f_{eq} and l_c and a fine-tuning relation $\varepsilon = \varepsilon_1(\Gamma)$.

An example of a configuration with two regular centers is presented in Fig. 7 for $\Gamma = 2$; the fine-tuned value of ε is $\varepsilon_1(2) = -0.3326\dots$, it belongs to the line $\varepsilon = \varepsilon_1(\Gamma)$.

The curve $\varepsilon = \varepsilon_1(\Gamma)$ in Fig. 1 has been obtained numerically. For small and large values of Γ , this fine-tuning relation can be derived analytically.

6.1.1. $\varepsilon_1(\Gamma)$ for weak gravity, $\Gamma \ll 1$

This derivation repeats the one for Eq. (49). The main difference is that we now obtain the value of $r(l)$ at the equator from (53) as

$$r_{eq} = r(l_{eq}) = \sqrt{2/|\varepsilon|}, \quad |\varepsilon| \ll 1, \tag{54}$$

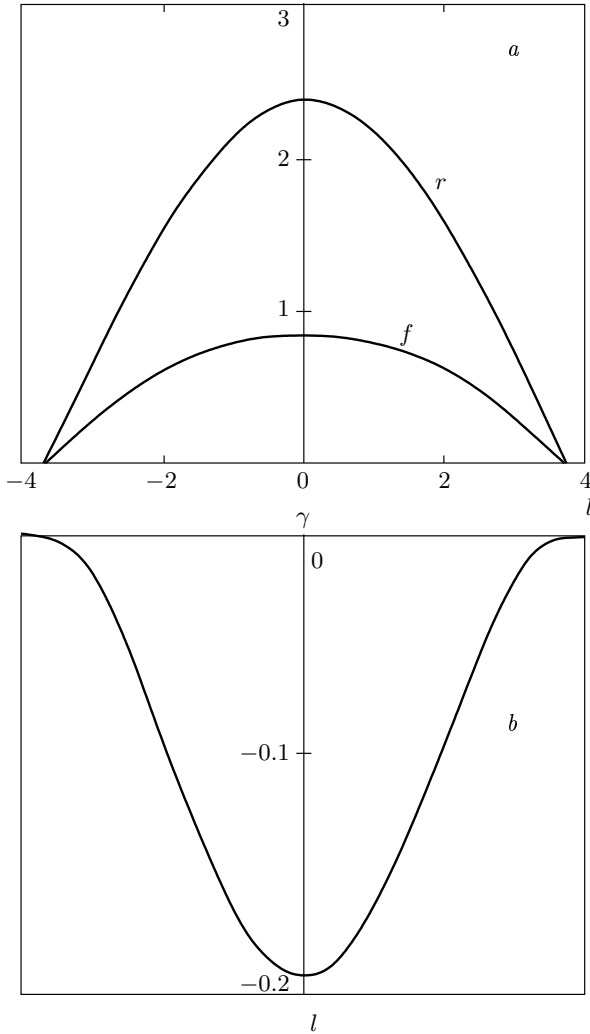


Fig. 7. An example of a configuration with two symmetric regular centers without knots of the scalar field: $\Gamma = 2$, the fine-tuned value $\varepsilon_1(2) = -0.3326\dots$; it belongs to the line $\varepsilon = \varepsilon_1(\Gamma)$; $r(l)$, $f(l)$ (a), and $\gamma(l)$ (b)

and use it instead of r_* . Substituting (54) in (47), we have

$$r'^2 = \Gamma \left(\ln \frac{2}{|\varepsilon|} - 2 \ln r - \frac{1}{d_0} - \frac{\varepsilon}{2d_0} r^2 \right),$$

$$\Gamma \ll 1, \quad 1 \ll r$$

instead of (48). In the intermediate region $1 \ll r \ll r_m$, this must coincide with (44). The resulting relation is

$$\varepsilon = -2 \exp \left(-\frac{1}{\Gamma} - \frac{1-J_1}{d_0} - 4J_2 \right) \approx -0.9e^{-1/\Gamma}, \quad (55)$$

$$\Gamma \ll 1.$$

6.1.2. $\varepsilon_1(\Gamma)$ for strong gravity, $\Gamma \gg 1$

Numerical integration shows that for $\Gamma \gg 1$, the scalar field f remains small in the whole interval between the centers, while $\psi = \varkappa \eta f$ is of the order of unity. Introducing λ in (36) as before and taking into account that $f \ll 1$, we again find Eqs. (37)–(39). It is convenient to integrate these equations from the equator to the center and to use boundary conditions in the form

$$\beta'(l_{eq}) = \psi'(l_{eq}) = \gamma'(l_{eq}) = 0, \quad \psi(l_{eq}) = \psi_{eq},$$

$$\beta(l_{eq}) = \frac{1}{2} \ln \frac{2\psi_{eq}^2}{2\psi_{eq}^2 - \lambda}. \quad (56)$$

The three parameters ψ_{eq} , $l_c - l_{eq}$, and λ are to be determined from the conditions

$$\psi(l_c) = 0, \quad r(l_c) = 0, \quad r'(l_c) = 1.$$

Numerical integration results in $\lambda = 1.9\dots$

For class-C solutions, the desired fine-tuning relation in the strong-gravity limit is

$$\varepsilon = -1 + 1.9/\Gamma. \quad (57)$$

6.2. Odd and even scalar fields

In the above solutions, the scalar field $f(l)$ without knots is an even function.

Because $f(l)$ may change its sign between the centers, there are two possibilities. If the number of knots of $f(l)$ is even, then $f(l)$ is an even function, reaching an extremum at the equator, and $f'(l_{eq}) = 0$. On the other hand, $f(l)$ with an odd number of knots is an odd function: $f(l_{eq}) = 0$, and $f'(l)$ is then an even function having an extremum at $l = l_{eq}$.

Numerical integration of Eqs. (13)–(15) in the case of an even number of knots can be performed with the same boundary conditions (56) as without knots. The results are displayed in Figs. 8–10.

Figure 8 shows a few solutions for the scalar field $f(l)$ with two knots and the corresponding functions $r(l)$.

Figure 9 shows the function $\gamma(l)$ in the whole range of l and in a close vicinity of the equator for visual clarity to demonstrate a minimum at the equator. We recall that γ enters the equations only via γ' and γ'' , and therefore, without loss of generality, we have set $\gamma(l_{eq}) = 0$ in Fig. 9b. The larger is Γ , the deeper is the local minimum of γ at the equator. Altogether, the gravitational potential has three minima: one at the equator and two others near the regular centers.

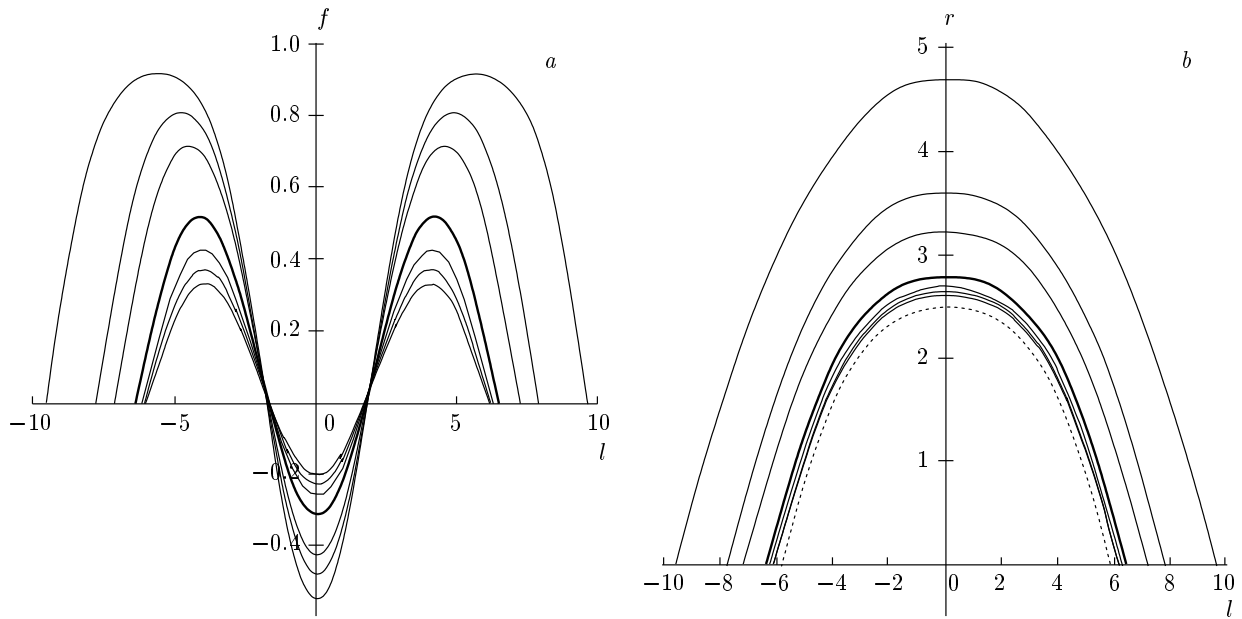


Fig. 8. Solutions with two symmetric centers with two knots of $f(l)$ for $\Gamma = 0.5, 0.75, 1, 2, 3, 4,$ and 5 in the order of decreasing amplitude; the corresponding fine-tuned values of ε are $-0.51275, -0.62765, -0.7019, -0.8365, -0.888, -0.9146,$ and -0.93115 ; $f(l)$ (a), $r(l)$ (b); the additional dashed curve corresponds to the limit $\Gamma \rightarrow \infty$

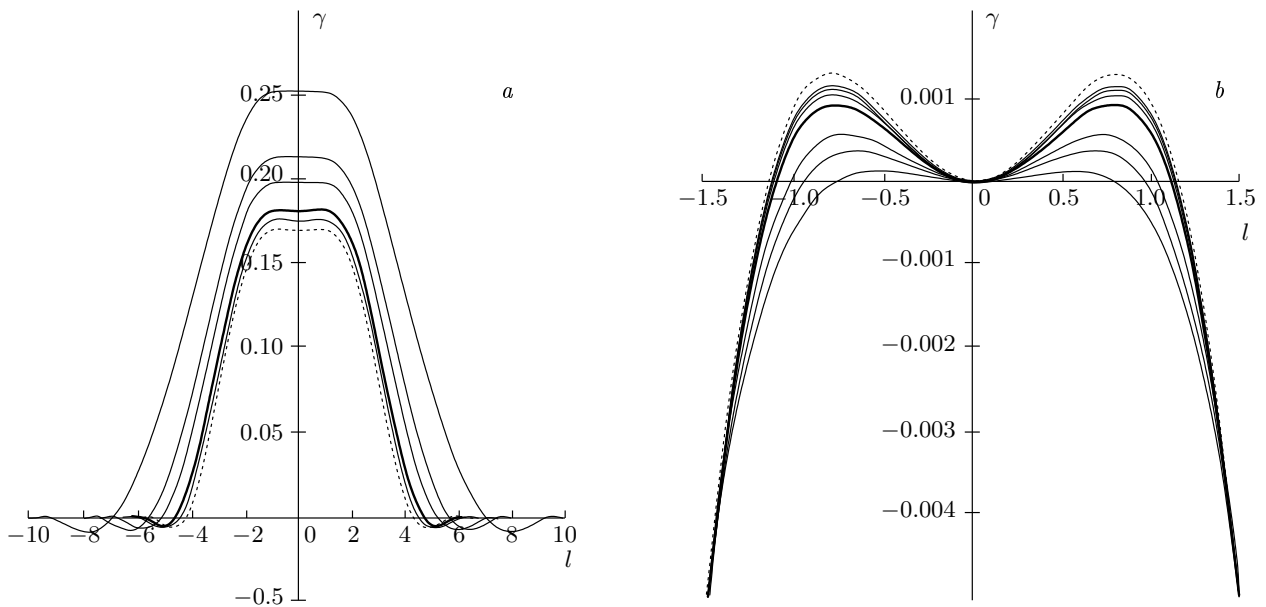


Fig. 9. The functions $\gamma(l)$ in the whole range of l (a) and in a close vicinity of the equator (b) for solutions with the same set of parameters as in Fig. 8

The fine-tuning relation $\varepsilon_3(\Gamma)$ for solutions with two knots of $f(l)$, found numerically, is shown in Fig. 10. Each curve in Figs. 8 and 9 corresponds to a point on this curve.

In solutions with an odd number of knots of $f(l)$, we have $f(l_{eq}) = 0$, and it follows from Eq. (16) that

$$f'^2 = \frac{\varepsilon + 1}{2}$$

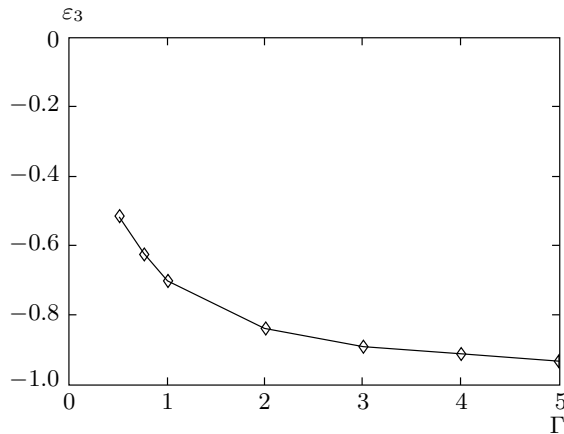


Fig. 10. The fine-tuning relation $\varepsilon_3(\Gamma)$ for solutions with two knots of $f(l)$ between the centers, displayed in Figs. 8 and 9

at the equator. For numerical integration of Eqs. (13)–(15) in this case, it is convenient to use the boundary conditions

$$\begin{aligned} \beta'(l_{eq}) = f(l_{eq}) = \gamma'(l_{eq}) = 0, \quad \beta(l_{eq}) = \beta_{eq}, \\ f'(l_{eq}) = \sqrt{(\varepsilon + 1)/2}. \end{aligned} \quad (58)$$

Then the three conditions $f(l_c) = 0$, $r(l_c) = 0$, and $r'(l_c) = 1$ determine the values of β_{eq} and $l_c - l_{eq}$ as well as the fine-tuning relation ($\varepsilon = \varepsilon_2(\Gamma)$ in the case of one knot). As an example, in Fig. 11, we present a numerical solution with one knot for $\Gamma = 2$, corresponding to $\varepsilon = -0.71$. Figure 11a shows $r(l)$ and $f(l)$; $\gamma(l)$ is depicted on Fig. 11b. The function $\gamma(l)$ is symmetric with respect to the equator and has two minima close to the centers.

We note that if we include configurations with angular deficits and excesses at the centers into consideration, then the existence of solutions with two centers is not restricted to particular lines in the (ε, Γ) plane. There is then a whole area of such solutions, bounded by

$$\varepsilon = \min(\varepsilon_*(\Gamma), -1)$$

from below and by the line $\varepsilon = \varepsilon_h(\Gamma)$ from above. Among the nonsymmetric solutions of this kind with several knots of the scalar field, we can find those with multiple local maxima and minima of $\gamma(l)$. Their possible connection with matter trapping and the hierarchy problem is discussed below.

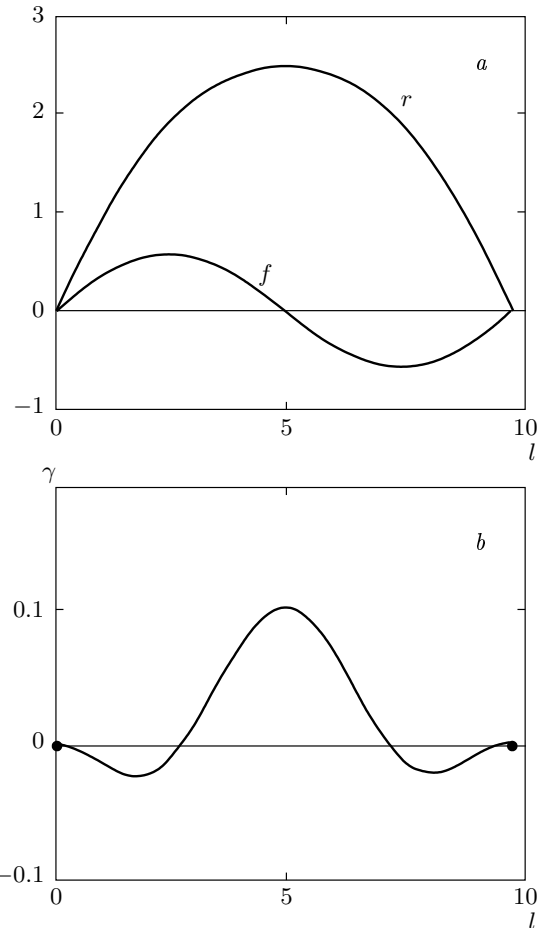


Fig. 11. Example of a solution with two symmetric regular centers and an odd scalar field with one knot; $\Gamma = 2$, the corresponding fine-tuned value $\varepsilon_2(\Gamma) = -0.71$; $r(l)$, $f(l)$ (a), and $\gamma(l)$ (b)

7. MATTER IN THE BACKGROUND OF GLOBAL STRING CONFIGURATIONS

In this section, we discuss the problem of trapping of classical point-like particles and test scalar fields by the gravitational field of the global string configurations described above.

7.1. Classical particles

The motion of classical particles in the bulk can be equivalently described in terms of geodesics or the Hamilton–Jacobi equation. We here use the second approach.

The Hamilton–Jacobi equation for a point-like test particle of (primary) mass m_0 in space–time with metric (10) is

$$e^{-2\gamma(l)} \left[\left(\frac{\partial S}{\partial t} \right)^2 - \left(\frac{\partial S}{\partial \mathbf{x}} \right)^2 \right] - \left(\frac{\partial S}{\partial l} \right)^2 - \frac{1}{r^2(l)} \left(\frac{\partial S}{\partial \theta} \right)^2 - m_0^2 = 0.$$

The metric is homogeneous with respect to all coordinates except l , and the action can be written as

$$S = Et - \mathbf{p}\mathbf{x} + S_l(l) + M\theta, \tag{59}$$

where E is the particle energy, \mathbf{p} is the particle momentum along the coordinates x^i , $i = 1, d_0 - 1$, θ is the angular coordinate in the extra dimensions (we note that $d\Omega^2 = d\theta^2$ for $d_1 = 1$) and M is its conjugate angular momentum. The remaining unknown function $S_l(l)$ satisfies the equation

$$\frac{dS_l}{dl} = \pm \sqrt{p^2 e^{-2\gamma(l)} - \frac{M^2}{r^2(l)} - m_0^2},$$

where

$$p^2 = E^2 - \mathbf{p}^2.$$

Zeros of the square root determine the turning points of classical motion.

We consider a particle with $M = 0$, i.e., moving in the bulk along the coordinate l (strictly to or from a brane if the brane is located at fixed l). Classical motion is allowed where the square root is real. The turning points l_t are determined by the equation

$$p^2 e^{-2\gamma(l_t)} - m_0^2 = 0.$$

If there is a minimum of $\gamma(l)$ at some $l = l_0$, a classical particle with

$$p^2 = m_0^2 e^{2\gamma(l_0)}$$

cannot move along the l direction and is trapped precisely at the minimum of γ . Particles with slightly larger p^2 can move between two turning points in the vicinity of l_0 . If it is a global minimum of γ , particles with any

$$p^2 \geq m_0^2 e^{2\gamma(l_0)}$$

are trapped.

It can also be verified that particles with the same value of p^2 but $M \neq 0$ (moving in the θ direction) have a still narrower range of motion along l .

In particular, near the equator of a configuration with two centers and three half-waves of ϕ (see Fig. 9), the turning points of finite classical motion exist for $\gamma(l_{eq}) < \gamma < \gamma_m$, where γ_m is the maximum of $\gamma(l)$. Setting

$$m_{eq}^2 = m_0^2 e^{2\gamma(l_{eq})},$$

we see that a classical particle is trapped near the equator if its energy is restricted by

$$m_{eq}^2 < p^2 < m_{eq}^2 \exp\{2[\gamma_m - \gamma(l_{eq})]\}.$$

It moves along the Minkowski coordinates as a free particle of mass m_{eq} .

7.2. Scalar fields

We consider a test scalar field χ with the Lagrangian L_χ such that

$$2L_\chi = \partial^A \chi^* \partial_A \chi - m_0^2 \chi^* \chi \tag{60}$$

in the background of our string configurations with metric (10). Here, the asterisk as a superscript denotes complex conjugation and m_0 is the initial field mass. The χ field satisfies the Klein–Gordon equation

$$\partial_A (\sqrt{g} g^{AB} \partial_B \chi) + \sqrt{g} m_0^2 \chi = 0, \tag{61}$$

where

$$g = |\det(g_{AB})| = \exp(2d_0\gamma + 2\beta).$$

Taking the symmetry of the problem into account, we can take a single mode of χ , assuming

$$\chi(x^A) = X(l) e^{-ip_\mu x^\mu} e^{in\theta}, \tag{62}$$

where $p_\mu = (E, \mathbf{p})$ is the ($d_0 = 4$)-momentum along the brane and n is an integer. Then $X(l)$ satisfies the equation

$$X'' + (d_0\gamma' + \beta')X' + (p^2 e^{-2\gamma} - n^2 e^{-2\beta} - m_\chi^2)X = 0, \tag{63}$$

where

$$p^2 = p_\mu p^\mu = E^2 - \mathbf{p}^2$$

is the effective mass squared, observed on the brane.

As a trapping criterion for a mode X , it is reasonable to require the finiteness of the χ -field energy E_χ per unit area of the brane,

$$E_\chi = \int T_t^t[\chi] \sqrt{g} d\theta dl = 2\pi \int T_t^t[\chi] \sqrt{g} dl < \infty, \tag{64}$$

where

$$T_t^t[\chi] = \frac{1}{2} \times [e^{-2\gamma}(E^2 + \mathbf{p}^2) + X'^2 + (n^2 e^{-2\beta} + m_0^2)X^2] \tag{65}$$

is the temporal component of the χ -field stress–energy tensor. We notice that the validity of Eq. (64) automatically guarantees finiteness of the norm $\int \sqrt{g} \chi^* \chi dl d\theta$

of the χ field considered as a quantum-mechanical wave function.

The finiteness of E_χ in the background of different regular configurations with infinite extra dimensions described above depends on the behavior of solutions of Eq. (63) at small and large l .

We begin with considering the χ -field behavior near a regular center $l = 0$, which is common to all classes of regular configurations. At small l , we have $e^\beta \equiv r \sim l$ and $\gamma \rightarrow 0$. Hence, Eq. (63) takes the approximate form

$$lX'' + X' + l(p^2 - m_0^2)X = 0, \quad n = 0, \quad (66)$$

$$lX'' + X' - (n^2/l)X = 0, \quad n \neq 0. \quad (67)$$

Equation (66) is solved by zeroth-order cylindrical functions if $p^2 \neq m_0^2$ and in elementary functions if $p^2 = m_0^2$; Eq. (67) is an Euler equation. At small l , the solutions behave as

$$\begin{aligned} X &\approx C_1 + C_2 \ln l, \quad n = 0, \\ X &\approx C_3 l^n + C_4 l^{-n}, \quad n \neq 0, \end{aligned} \quad (68)$$

with integration constants C_i . To make the integral in (64) converge as $l \rightarrow 0$, we must choose $C_2 = 0$ and $C_4 = 0$, i.e., only one of the two linearly independent solutions in each case.

We now consider the asymptotic form of solutions of Eq. (63) as $l \rightarrow \infty$ for different background configurations.

A1: at large l , $\gamma \sim \beta \sim hl$, $h = \text{const} > 0$. In Eq. (63), the terms with p^2 and m^2 are negligible, and the solution has the asymptotic form

$$\begin{aligned} X &\approx C_+ e^{-a+l} + C_- e^{-a-l}, \\ 2a_\pm &= (D-1)h \pm \sqrt{(D-1)^2 h^2 + 4m_0^2}, \end{aligned} \quad (69)$$

where C_\pm are integration constants and $D = d_0 + 2$ is the total space-time dimension. It is easy to verify that criterion (64) holds for solution with $C_+ \neq 0$, $C_- = 0$. Hence, scalar fields with any nonzero mass can be trapped on such branes.

A2: at large l , $e^{d_0\gamma} \sim e^\beta \sim l$. Again, the terms with p^2 and m^2 are negligible, and Eq. (63) transforms to

$$X'' + 2X'/l - m_0^2 X = 0,$$

whose solution is

$$X \approx \frac{C_+ e^{m_0 l} + C_- e^{-m_0 l}}{l}, \quad (70)$$

and evidently the solution with $C_+ = 0$ satisfies criterion (64).

B1: at large l , $r \equiv e^\beta \rightarrow r_*$, $\gamma \approx -hl$, $h > 0$, and the approximate form of Eq. (63) is

$$X'' - d_0 h X' + p^2 e^{2hl} X = 0. \quad (71)$$

For $p \neq 0$, it is solved in cylindrical functions, the general solution being

$$\begin{aligned} X &= e^{d_0 hl/2} Z_{d_0/2} \left(\frac{|p|}{h} e^{hl} \right) \sim \\ &\sim e^{(d_0-1)hl/2} \sin \left(\frac{|p|}{h} e^{hl} + \Phi \right), \end{aligned} \quad (72)$$

where Φ is a constant phase. It is easy to verify that E_χ diverges as $\int e^{hl} dl$. Therefore, massive modes with any $p^2 > 0$ are not trapped by B1 configurations.

B2: at large l , $r \rightarrow r_*$ and $\gamma \approx hl$, $h > 0$. The situation is almost the same as in case A1; the solution of Eq. (63) has asymptotic form (69) with the replacements

$$D - 1 \mapsto d_0, \quad m_0^2 \mapsto m_0^2 + n^2/r_*^2.$$

Again, only the solution with $C_- = 0$ provides convergence of E_χ .

Thus, the configurations of classes A1, A2, and B2 can trap massive scalar modes; at both large and small l , only one of the two linearly independent solutions of Eq. (63) is selected, and therefore we have a boundary-value problem with a discrete spectrum of p^2 for any given values of m_0 , n and the background parameters.

7.3. The Schrödinger equation

It is helpful to reformulate the boundary-value problem for scalar field modes in terms of the Schrödinger equation. For this, we make the following substitutions in (63):

$$dl = e^\gamma dx, \quad X(l) = \frac{y(x)}{\sqrt{f(x)}}, \quad (73)$$

where

$$f(x) = \exp((d_0 - 1)\gamma + \beta).$$

The new variable x is actually an analogue of the well-known ‘‘tortoise coordinate’’ in the analysis of spherically symmetric metrics, such that the metric takes the form

$$ds^2 = e^{2\gamma} (\eta_{\mu\nu} dx^\mu dx^\nu - dx^2) - e^{2\beta} d\theta^2. \quad (74)$$

Then Eq. (63) transforms to the Schrödinger form

$$y_{xx} + [p^2 - V_{eff}(x)]y = 0 \quad (75)$$

with the effective potential

$$V_{eff} = (m_0^2 + n^2 e^{-2\beta}) e^{2\gamma} + \frac{f_{xx}}{2f} - \frac{f_x^2}{4f^2}, \quad (76)$$

where the subscript x denotes d/dx . We recall that the eigenvalue p^2 is the effective mass squared, observed in Minkowski space.

Near the center (without loss of generality, $x \approx l \rightarrow 0$), we have

$$V_{eff} \approx \frac{n^2}{x^2} + m_0^2 + \frac{1}{4} \left[1 + 2(d_0 - 1)\gamma_{xx} + \beta_{xx} \right]_{x=0}. \quad (77)$$

For $n \neq 0$, it is therefore a potential well, whereas $V_{eff} \rightarrow \text{const}$ for $n = 0$.

At large l for different backgrounds, we have:

A1: $x \rightarrow x_+ < \infty, \quad x_+ - x \sim e^{-hl}, \quad h > 0,$

$$V_{eff}(x) \approx e^{2hl} \left[m_0^2 + \frac{h^2}{4}(d_0^2 + 2d_0) \right]; \quad (78)$$

A2: $x \sim l^{(d_0-1)/d_0} \rightarrow \infty,$

$$V_{eff}(x) \approx m_0^2 e^{2\gamma} \sim l^{2/d_0} \sim x^{2/(d_0-1)}; \quad (79)$$

B1: $x \sim e^{hl} \rightarrow \infty, \quad h > 0,$

$$V_{eff}(x) \approx e^{-2hl} \left[m_0^2 + \frac{n^2}{r_*^2} + \frac{h^2}{4}(d_0^2 - 1) \right] \sim \frac{1}{x^2}; \quad (80)$$

B2: $x \rightarrow x_* < \infty, \quad x_* - x \sim e^{-hl}, \quad h > 0,$

$$V_{eff}(x) \approx e^{2hl} \left[m_0^2 + \frac{n^2}{r_*^2} + \frac{h^2}{4}(d_0^2 - 1) \right]. \quad (81)$$

We see that in cases A1, A2, and B2, the potential increases to infinity at large l , which leads to discrete spectra of p^2 . For B1 configurations (with a horizon at $l = \infty$), in the standard quantum mechanics, we would expect a continuous spectrum of states; in our case, with the appropriate boundary conditions, as we saw above, there are no admissible states with $p^2 > 0$.

7.4. Massless modes in configurations with infinite extra dimensions

For a possible massless mode,

$$p^2 = m_0^2 = n^2 = 0,$$

Eq. (63) is easily solved as

$$\begin{aligned} X' &= C_1 e^{-d_0\gamma - \beta} dl, \\ X &= C_1 \int e^{-d_0\gamma - \beta} + C_2, \quad C_{1,2} = \text{const}, \end{aligned} \quad (82)$$

and X is found by quadrature.

One of the solutions is $X = \text{const}$. It is easy to verify that with this solution, which is well-behaved at a regular center, the energy E_χ in Eq. (64) diverges at large l in the backgrounds A1, A2, and B2, but converges in the background B1.

For the other solution with $C_1 \neq 0$, on the contrary, E_χ converges at large l in the backgrounds A1, A2, and B2 and diverges in B1. This solution, however, is singular at the center and leads to a divergence in E_χ there.

Thus, B1 configurations with horizons, being unable to trap massive scalar fields, are the only ones that can trap a massless scalar.

8. CONFIGURATIONS WITH TWO CENTERS AND THE HIERARCHY PROBLEM

In configurations with two symmetric regular centers and two knots of the scalar field, there are three minima of the “gravitational potential” γ (see Fig. 9). The minimum at the equator is higher than the other two located near the centers. A similar (and even more complicated) structure may be expected for configurations with a larger number of scalar-field knots. The minima of γ are able to trap classical particles. As regards quantum particles (at least spinless), effective potential (76) not necessarily has a minimum precisely where γ has a minimum, and an additional detailed study is necessary. Nevertheless, semiclassically at least, quantum and classical particles must be trapped in close positions, and the main difference between them is that quantum particles can tunnel from a higher minimum of V_{eff} to a lower one.

We now suppose that a particle described by a certain mode of the χ field (for simplicity, with $n = 0$) is trapped at some position l_i . Mode equation (63) can then be rewritten as

$$(\sqrt{g}X')' + \sqrt{g}X e^{-2\gamma} p^2 = \sqrt{g}m_0^2 X. \quad (83)$$

We integrate this equation over the extra dimension from one center to the other. We have

$$\int (\sqrt{g}X')' dl = 0$$

because

$$\sqrt{g} = r e^{d_0\gamma}$$

is zero at both centers. For a particle trapped at some fixed position $l = l_i$, we obtain

$$p^2 = m_i^2 = m_0^2 \frac{\int \sqrt{g} X dl}{\int \sqrt{g} e^{-2\gamma} X dl} \approx m_0^2 e^{2\gamma(l_i)}. \quad (84)$$

To interpret this result, we note that the entire picture looks quite different depending on the size of the extra dimensions, characterized by the distance l_c between the centers. This size, in turn, varies with the value of $\Gamma = \kappa^2 \eta^2$: it is close to unity (i.e., the length unit, which is also arbitrary) for large Γ and tends to infinity as $\Gamma \rightarrow 0$. For (comparatively) weak gravity of the string, $\Gamma \rightarrow 0$, when l_c is very large, all minima of $\gamma(l)$ form individual branes located in the bulk far from one another. In this case, an observer located on one of the branes sees only particles corresponding to modes trapped on this brane; tunneling from one brane to another is then seen as the appearance or disappearance of observable particles. The entire picture may be used for treating the interaction hierarchy problem in the spirit of Randall–Sundrum first model [4].

In the opposite case $\Gamma \rightarrow \infty$ (if the unit length $(\lambda_0 \eta)^{-1/2}$ is also sufficiently small), l_c can be a length invisible for modern instruments, e.g., $l_c \ll 10^{-17}$ cm. We then arrive at a picture close to the original Kaluza–Klein concept; particles with the same primary mass m_0 , being trapped at different minima of the effective potential, are seen as particles with different masses, and the tunneling process from a higher minimum to a lower one is observed as a decay of a particle of a larger mass to that of a smaller mass, with energy release in some form. This may be a natural explanation of the existing families of particles with different masses but similar other properties. A more detailed study of this possibility is desirable but is beyond the scope of the present paper.

9. CONCLUSION

Our phenomenological approach based on the macroscopic theory of phase transitions with spontaneous symmetry breaking allows studying the general physical properties of topological defects in the framework of the brane-world concept. In particular, in this paper, we have studied the gravitational properties of global strings located in extra dimensions. We have given a general description and classification of possible regular solutions and presented a map showing the location of different solutions in the space of physical parameters.

Among the variety of regular solutions, there are ones having brane features, including solutions with

multiple branes, as well as those of potential interest from the standpoint of the hierarchy problem.

In connection with branes, we have analyzed the possibilities of trapping of classical particles and scalar fields. We have shown that contrary to the domain-wall case, in the case of an extra-dimensional global string, matter can be trapped by gravity even without coupling to the scalar field that forms the string itself.

Among the configurations with two centers, the structures having several minima of $\gamma(l)$ may be interesting in connection with the hierarchy problem. If the distance between the centers is small, we work within the Kaluza–Klein concept, and the same particle, being trapped at different minima, looks to an observer as a family of similar particles with different rest masses.

We appreciate partial financial support from the RFBR (projects №№ 05-02-17478 and 07-02-13614-ofts).

REFERENCES

1. T. Kaluza, *Sitzungsber. Preuss. Akad. Wiss. Berlin, Math. Phys.* **K1**, 966 (1921); O. Klein, *Z. Phys.* **37**, 895 (1926).
2. K. Akama, *Lect. Notes Phys.* **176**, 267 (1982); V. A. Rubakov and M. E. Shaposhnikov, *Phys. Lett. B* **125**, 136 (1983); M. Visser, *Phys. Lett. B* **159**, 22 (1985); E. J. Squires, *Phys. Lett. B* **167**, 286 (1986); G. W. Gibbons and D. L. Wiltshire, *Nucl. Phys. B* **717**, (1987).
3. P. Horava and E. Witten, *Nucl. Phys. B* **460**, 506 (1996); **475**, 94 (1996); E. Witten, *Nucl. Phys. B* **471**, 135 (1996).
4. L. Randall and R. Sundrum, *Phys. Rev. Lett.* **83**, 3370 (1999).
5. B. Acharya, K. Bobkov, G. Kane, P. Kumar, and D. Vaman, E-print archives, hep-th/0606262; G. Burdman, E-print archives, hep-ph/0703194; S. Das, A. Dey, and S. SenGupta, *Class. Quant. Grav.* **23**, L67-72 (2006); E-print archives, hep-th/0511247; P. Chen, E-print archives, hep-ph/0611378; S. Das, A. Dey, and S. SenGupta, E-print archives, gr-qc/0610021; T. Biswas and A. Notari, E-print archives, hep-ph/0511207; G. Cognola, E. Elizalde, S. Nojiri, S. D. Odintsov, and S. Zerbini, E-print archives, hep-th/0601008; S. Das, A. Dey, and S. SenGupta, E-print archives, hep-th/0704.3113; C. S. Lim, N. Maru, and K. Hasegawa, E-print archives, hep-th/0605180.

6. D. A. Kirzhnits, *Pis'ma Zh. Eksp. Teor. Fiz.* **15**, 745 (1972).
7. Ya. B. Zel'dovich, I. Yu. Kobzarev, and L. B. Okun', *Zh. Eksp. Teor. Fiz.* **67**, 3 (1974).
8. O. DeWolfe, D. Z. Freedman, S. S. Gubser, and A. Karch, *Phys. Rev. D* **62**, 046008 (2000); E-print archives, hep-th/9909134.
9. M. Gremm, *Phys. Rev. D* **62**, 044017 (2000); A. Davidson and P. D. Mannheim, E-print archives, hep-th/0009064; C. Csaki, J. Erlich, T. J. Hollowood, and Y. Shirman, *Nucl. Phys. B* **581**, 309 (2000); D. Ba-zeia, F. A. Brito, and J. R. Nascimento, *Phys. Rev. D* **68**, 085007 (2003).
10. S. Kobayashi, K. Koyama, and J. Soda, *Phys. Rev. D* **65**, 064014 (2002).
11. A. Melfo, N. Pantoja, and A. Skrzewski, *Phys. Rev. D* **67**, 105003 (2003).
12. R. Ghoroku and M. Yahiro, E-print archives, hep-th/0305150.
13. K. A. Bronnikov and B. E. Meierovich, *Grav. & Cosmol.* **9**, 313 (2003); E-print archives, gr-qc/0402030.
14. S. T. Abdyrakhmanov, K. A. Bronnikov, and B. E. Meierovich, *Grav. & Cosmol.* **11**, 82 (2005); E-print archives, gr-qc/0503055.
15. I. Olasagasti and A. Vilenkin, *Phys. Rev. D* **62**, 044014 (2000); E-print archives, hep-th/0003300.
16. E. Roessl and M. Shaposhnikov, *Phys. Rev. D* **66**, 084008 (2002); E-print archives, hep-th/0205320.
17. K. A. Bronnikov and B. E. Meierovich, *Zh. Eksp. Teor. Fiz.* **128**, 1184 (2005); E-print archives, gr-qc/0507032.
18. K. A. Bronnikov, B. E. Meierovich, and S. T. Abdyrakhmanov, *Grav. & Cosmol.* **12**, 109 (2006).
19. I. I. Kogan, S. Mouslopoulos, A. Papazoglou, and G. Ross, E-print archives, hep-th/0107086; R. Koley and S. Kar, *Class. Quantum Grav.* **24**, 79 (2007); G. Kofinas and T. N. Tomaras, E-print archives, hep-th/0702010; S. Kanno and J. Soda, E-print archives, hep-th/0404207.
20. K. Benson and I. Cho, E-print archives, hep-th/0104067.
21. I. Cho and A. Vilenkin, E-print archives, gr-qc/9708005.
22. Y. Brihaye and T. Delsate, *Class. Quantum Grav.* **24**, 1279 (2007).
23. J. M. Cline, J. Descheneau, M. Giovannini, and J. Vinet, E-print archives, hep-th/0304147v2.